Journal of Cellular Biochemistry 101:89–98 (2007)

Tissue-Specific Expression of Riken 2810430M08 and its Function in T-Cell Immune Responses

Tao Wu,[1,2] ShenJiang Hu,[1] Xiaoying Qiao,[2] Hongyu Luo,[2]* and Jiangping Wu[2,3,4]*

[1]Institute of Cardiology, the First Affiliated Hospital, Zhejiang University, Hangzhou, China
[2]The Laboratory of Immunology, Centre hospitalier de l'Université de Montréal (CHUM), Notre Dame Hospital, Montreal, Quebec, Canada
[3]College of Medicine, Zhejiang University, Hangzhou, China
[4]Nephrology Service, Centre hospitalier de l'Université de Montréal (CHUM), Notre Dame Hospital, Montreal, Quebec, Canada

Abstract Riken 2810430M08 is a gene with unknown functions. According to in situ hybridization (ISH), it presented a pattern of temporal expression, peaking in the mid-gestation (embryonic Days e9–e14) stage in most tissues. In the late-gestation stage and during the adulthood, Riken 2810430M08 was expressed in some tissues with and without a robust proliferation program. Thus, the gene might have important functions that are related and unrelated to proliferation. Its expression was induced after T-cell receptor stimulation in T cells. However, transgenic mice with actin promoter-driven expression of Riken 2810430M08 showed normal in vitro and in vivo T cells responses, such as fetal thymus development, adult T cells activation marker expression, lymphokine secretion, proliferation and migration, and delayed type hypersensitivity (DTH). The expression of Riken 2810430M08 during ontogeny has provided useful clues for further investigation. Additional studies are warranted to examine its role in immune and other systems. J. Cell. Biochem. 101: 89–98, 2007.

Key words: Riken 2810430M08; in situ hybridization; transgenic; T-cell

To elucidate the molecular mechanisms of T-cell activation and differentiation, we conducted DNA microarray analysis, employing the mouse 15,000 cDNA panel of the National Institute of Aging, USA, to compare gene expression patterns of resting versus activated T cells (anti-CD3 and -CD28 stimulation for 24 h). Riken 2810430M08 was one of the genes found to undergo significant changes after activation. So far, Riken 2810430M08 remains a gene with unknown functions. Its cDNA sequence has no significant homology with other known genes, and its peptide sequence carries no conserved domains with proven function. The tissue-specific expression of Riken 2810430M08 has not been investigated.

In this study, we mapped the Riken 2810430M08 expression pattern during ontogeny, and conducted detailed in vitro and in vivo investigations of its functions in the T-cell compartment of the immune system, using transgenic (Tg) mice with actin promoter-driven Riken 2810430M08 expression.

MATERIALS AND METHODS

In Situ Hybridization (ISH)

Mouse Riken 2810430M08 full-length cDNA (1,040 bp) in pCMV-SPORT6 (clone MGC-8134; American Type Culture Collection, Rockville, MD) was employed to generate sense and antisense riboprobes, using SP6 and T7 RNA polymerase for both ^{35}S-UTP and ^{35}S-CTP incorporation [Marcinkiewicz, 2002].

Grant sponsor: CIHR; Grant numbers: MOP57697, MOP69089, MOP79565; Grant sponsor: The Kidney Foundation of Canada; Grant sponsor: The Heart and Stroke Foundation of Quebec; Grant sponsor: The Juvenile Diabetes Research Foundation, USA; Grant number: 1-2005-197; Grant sponsor: The J.-Louis Levesque Foundation; Grant sponsor: FRSQ.

*Correspondence to: Dr. H. Luo or J. Wu, Laboratory of Immunology, Research Centre, CHUM, Notre Dame Hospital, Pavilion DeSève, Room Y-5616, 1560 Sherbrooke Street East, Montreal, Que., Canada H2L 4M1. E-mail: hongyu.luo@umontreal.ca or jianping.wu@umontreal.ca

Received 1 May 2006; Accepted 6 September 2006

DOI 10.1002/jcb.21170

Tissues were frozen in −35°C isopentane and kept at −80°C, until sectioned. ISH was performed on 10-μm thick cryostat-cut slices, as outlined previously [Marcinkiewicz, 2002]. Anatomic ISH was conducted with X-ray films. ISH microscopy was undertaken with 8-day exposure of photographic emulsion. The slides were developed and then counter stained with hematoxylin.

Northern Blot Analysis

A partial Riken 2810430M08 cDNA fragment (clone H3016A11, National Institute of Aging, mouse 15K cDNA clone set; positions 16–960, according to the sequence in GeneBank, accession number BC006787) was labeled with a digoxin (Dig)-labeling kit from Roche Applied Sciences (Laval, Quebec, Canada). Total RNA was extracted from cultured cells with TRIzol (Invitrogen, Burlington, Ontario, Canada). RNA (20 μg/lane) was resolved in 0.9% formaldehyde-agarose gels and transferred to N-Hybond nylon membranes (Amersham Biosciences, Baie d'Urfe, Quebec, Canada). The membranes were hybridized with Dig-labeled probes, and the signals were revealed by a Dig detection kit (Roche Applied Sciences). Band intensities of 18S and 28S ribosomal RNA were indicators of even RNA loading.

Generation of Riken 2810430M08 Tg Mice

Mouse full-length Riken 2810430M08 cDNA (1,040 bp) was excised from pCMV-SPORT6 with SmaI/XbaI and cloned into the BamHI (blunted)/XbaI sites in vector pAC, between the human β-actin promoter and β-actin polyA signals. The resulting construct was named pAC-Riken 2810430M08. The 5.8-kb ClaI/ClaI fragment containing the β-actin promoter, Riken 2810430M08 cDNA and β-actin polyA signal was excised and injected into fertilized C3H × C57BL/6 eggs. Genotyping of the Tg mice was first performed by Southern blot analysis. Tail DNA of the founders (10 μg/mouse) was digested with PstI and resolved by 1% agarose gel electrophoresis. The DNA was transferred onto N^+ Hybond nylon membranes after denaturation. A 0.8-kb band, specific to the transgene was detected by the same Dig-labeled Riken 2810430M08 probe as was employed for Northern blot analysis. Subsequent genotyping was undertaken by PCR. The 5′ and 3′ primers were CTGCGAGATGATTTCATGATG and GAATGCAATTGTTGTTGGTAACTTG, respectively, to detect a 428-bp band. The following PCR condition was employed: 94°C × 5 min, 1 cycle; 94°C × 1 min, 55°C × 1 min, 72°C × 1 min, 30 cycles; 72°C × 5 min, 1 cycle.

Real-Time Reverse Transcription-Polymerase Chain Reaction (RT-PCR)

Riken 2810430M08 mRNA in Tg and wild type (WT) cells was measured by real-time RT-PCR; the 5′ and 3′ primers were GCTGATGTCAACTGTTTCC and CGCAGAATCTTCCACCCT, respectively. A 147-bp product was detected with the following amplification program: 95°C × 15 min, 1 cycle; 94°C × 15 s, 55°C × 30 s, 72°C × 30 s, 40 cycles.

β-actin mRNA levels were measured as internal controls; the 5′ and 3′ primers were TGGTACCACAGGCATTGTGAT and TGATGTCACGCACGATTTCCCT, respectively, with the same amplification program as for Riken 2810430M08 mRNA.

Real-time PCR was performed in triplicate, and the signal ratios of Riken 2810430M08/β-actin represented the normalized expression levels of these genes.

Flow Cytometry

CD4, CD8, CD3, and B220 expression in adult thymocytes and splenocytes was analyzed by flow cytometry. CD25 and CD69 expression in T cells was investigated by gating on Thy1.2 cells, as described in our previous publication [Luo et al., 2004]. Different stages of double negative (DN) populations of fetal thymocytes from embryonic Day 19 (E19) fetus were analyzed by CD25 and CD44 staining on Lin^- negative ($CD3^-CD4^-CD8^-B220^-NK1.1^-$) thymocytes [Terra et al., 2005].

Lymphokine Secretion and Proliferation

Adult spleen T cells were purified and cultured according to established methods [Luo et al., 2004]. They were stimulated with various reagents. In some experiments, total spleen cells were stimulated with mitomycin-C-treated BALB/c spleen cells in mixed lymphocyte culture. Cell supernatants were collected and assayed for IL-2, IFN-γ, and IL-4 by ELISA. To prepare total E17 embryonic cells, the head of the fetuses were first removed, and the bodies were minced to pieces of about 1 mm^3 in size. The tissues were then digested with 0.25% trypsin for 20 min at 37°C; the mix was centrifuged at 500*g*, and the supernatant was

discarded; fresh trypsin (0.25%) was added to the pellet and the digestion continued for additional 40 min with change of fresh trypsin (0.25%) every 10 min. The isolated fetal cells were cultured at 0.4×10^6 cells/200 μl/well in RPMI 1640 medium containing 10% FCS for 20 h. Fetal thymocytes from E19 embryos were cultured at 0.4×10^6/200 μl/well in RPMI 1640 medium containing 10% FCS for 20 h in 96-well plates. Cell proliferation was measured by ^{3}H-thymidine uptake, which has been detailed in our previous publication [Luo et al., 2004].

Measurement of Immunoglobulin Isotype Levels in Sera

Mouse serum Ig isotype levels were measured with Ig isotyping ELISA and OptEIA kits from BD Biosciences (Mississauga, Ontario, Canada), according to the manufacturer's instructions.

Delayed Type Hypersensitivity (DTH) Assay

Mice were first primed by painting their shaved abdominal skin with FITC. On Day 6, ear thickness was measured, and the ears were then challenged by FITC painting. Ear thickness was re-measured after 24 h on Day 7, and any increases were registered. This method has been described elsewhere [Luo et al., 2004].

In Vitro Lymph Node (LN) Cell Migration Assay

In vitro migration assays were performed in Transwell chambers (6.5 mm in diameter, 5 μm pore size; Costar Corp., Cambridge, MA), as detailed in our previous publication [Shi et al., 2003]. The lower chamber contained 600 μl serum-free medium in the presence of SDF-1α (80 ng/ml) from R & D Systems (Minneapolis, MN). The upper chamber held 100 μl serum-free medium containing 0.3×10^6 T cells. The Transwell ensemble was then incubated at 37°C for 2 h, and T cells migrating into the lower chamber were counted by flow cytometry. All the samples were in duplicate.

RESULTS

Riken 2810430M08 Expression During Ontogeny

Riken 2810430M08 expression during ontogeny and in adult tissues is not known. We employed ISH to map the Riken 2810430M08 expression pattern during ontogeny, starting from embryonic Day 9 (e9) and in adult organs, using an antisense probe derived from Riken 2810430M08 cDNA.

At mid-gestation (Days e9–e14), 2810430M08 mRNA was expressed in primordia of most organs (Fig. 1A). Very strong signals were present in the neuroepithelium (NE) (Fig. 1A, vertical bar, and Fig. 1C) and in the NE-derived neopalial cortex (NCx; Fig. 1E). At a later embryonic development stage starting from e17 to p1 (postnatal Day 1), there was a general decline of 2810430M08 mRNA levels in most organs (Fig. 1F,G), with the exception of the thymus, kidney, and skin.

Substantial remodeling of the 2810430M08 expression pattern occurred postnatally. On p10, appreciable 2810430M08 mRNA levels were found in the cerebellum and cortex of the brain, retina, thymus, submaxillary gland, skin, and testes (Fig. 1H,I).

2810430M08 mRNA in Adult Tissues

In the brain, significant 2810430M08 mRNA concentration was found in the hippocampus cornu ammonis area 1 and related dentate gyrus (Fig. 2A). Although less abundant, gray matter in other brain regions, for example, the amygdales or mammillary bodies displayed 2810430M08 labeling (Fig. 2A). In contrast, white matter regions, such as the corpus callosum containing oligodendrocytes, were not labeled (Fig. 2A). This was confirmed in the spinal cord where weak hybridization occurred in the central gray matter (Fig. 2B), but not in the white matter. At the cellular level, high 2810430M08 mRNA concentration was seen within the pyramidal neuron layer of CA1 in the hippocampus and in granule neurons of the DG (Fig. 2C). Neurons in the brain cortical region displayed moderate levels of 2810430 M08 signal (Fig. 2D). At higher magnification, the signal was present within cortical neurons (large arrows in Fig. 2E), but not supportive glial cells (small arrows in Fig. 2E). A discrete 2810430M08 signal was apparent in Purkinje cells in the cerebellum (arrows in Fig. 2F,G).

In the adrenal glands, noticeable 2810430M08 signals occurred within the marginal zone of the cortex, but not medulla (Fig. 3A). 2810430M08 mRNA was most abundant within testes seminiferous tubules (Fig. 3B). At higher magnification (Fig. 3C), most 2810430M08 mRNA was confined to spermatocytes (Sp). There was no detectable signal in cells lining the

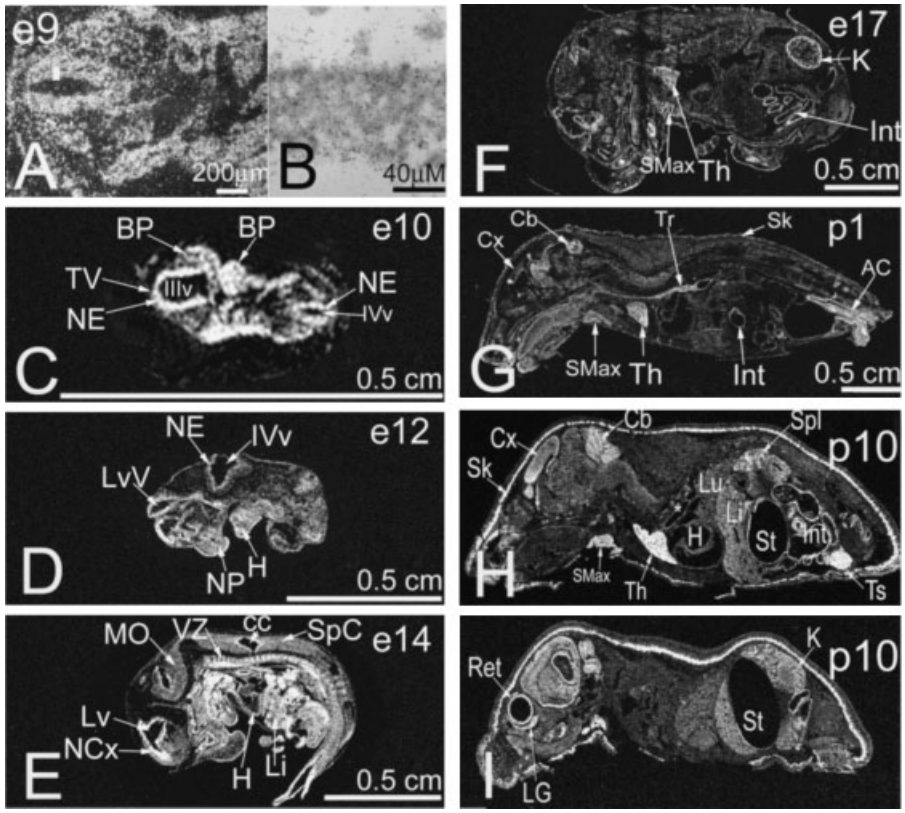

Fig. 1. Riken 2810430M08 expression during ontogeny according to in situ hybridization (ISH). Riken 2810430M08 ISH in mice from e9 to p10 is shown. IIIv, third ventricle; IVv, fourth ventricle; AC, anal canal; BP, brachial pouch; Cb, cerebellum; cc, the central canal of spinal cord; Cx, cerebral cortex; H, heart; Int, intestine; K, kidney; Lg, lacrimal gland; Li, liver; Lv, lateral ventricle; LvV, lateral ventricle vesicle; Lu, lung; MO, medulla oblongata; NCx, neopalial cortex; NE, neuroepithelium; NP, nasal process; Ret, retina; Sk, skin; SMax, submaxillary gland; SpC, spinal cord; Spl, spleen; St, stomach; Th, thymus; Tr, trachea; Ts, testis; TV, telencephalic vesicle; VZ, vertebrae zone. **A**, **C**–**I**: Dark-field X-ray autoradiograph images; **panels** H and I are two different planes of p10 whole body sections. **B**: The neuroepithelial cell layer by bright-field photo emulsion micrography. Ages are indicated.

periphery of the tubules, where Sertoli cells and spermatogonia reside. Leydig cells (LC) in the interstitium were unlabeled. A very strong signal was found in hair follicles, both in the internal (thin arrow) and external root sheaths, with a moderate level of signal present in the follicle matrix (Fig. 3D).

2810430M08 mRNA Expression in Adult Lymphoid Organs and T Cells

Adult lymphoid organs such as the thymus and spleen contained moderate levels of 2810430M08 mRNA (Fig. 3E,F). In the thymus, the cortex had stronger signals than the medulla, and in the spleen, the white pulp had stronger signals than the red pulp.

2810430M08 expression during T-cell activation was investigated by Northern blot analysis. Thymocytes and spleen T cells were stimulated with Con A and anti-CD3 (clone 2C11), respectively, and then harvested at 5 and 24 h. As shown in Figure 3G, one discrete band representing 2810430M08 mRNA below the 18S ribosome marker was detected in unstimulated cells; its intensity increased after 5 h, followed by a decline at 24 h.

Generation of 2810430M08 Tg Mice

Tg mice expressing human β-actin promoter-driven 2810430M08 were generated to study 2810430M08 functions. The plasmid construct for Tg mice generation is illustrated in Figure 4A. Two Tg founders (lines 5154 and 8735) were identified by Southern blot analysis, which revealed 0.8-kb bands specific to Tg mice (Fig. 4B). PCR was performed for routine genotyping of Tg mice; Tg, but not WT tail DNA displayed a 428-bp band (Fig. 4C).

Increased 2810430M08 mRNA expression in mature spleen T cells was confirmed by

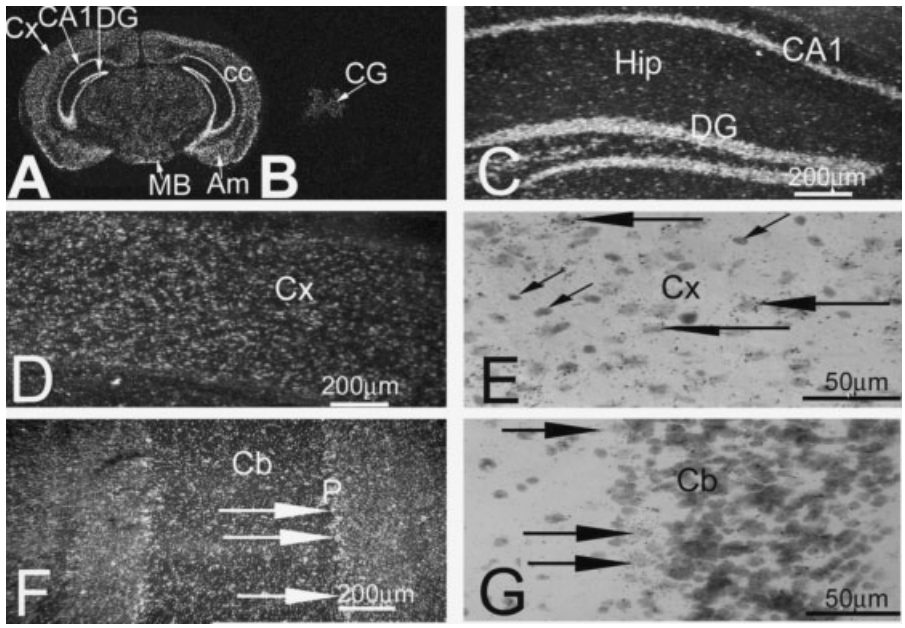

Fig. 2. ISH of selected adult brain areas for Riken 2810430M08 expression. **A**: Brain coronal section. AM, amygdala; CA1, hippocampal area 1; cc, central canal of the spinal cord; Cx, cortex; DG, dentate gyrus; MB, mammillary bodies. **B**: Spinal cord coronal section. CG, central gray matter area. **C**: Higher magnification of the area around the hippocampus (Hip). **D**, **E**: Higher magnification of the cortex (Cx). Large arrows indicate positively labeled neurons, and small arrows, unlabeled glial cells. **F**, **G**: Higher magnification of the cerebellum (Cb). Arrows indicate labeled Purkinje (P) cells. A–D, F: Dark-field X-ray autoradiography; E, G: Bright-field photo emulsion micrography.

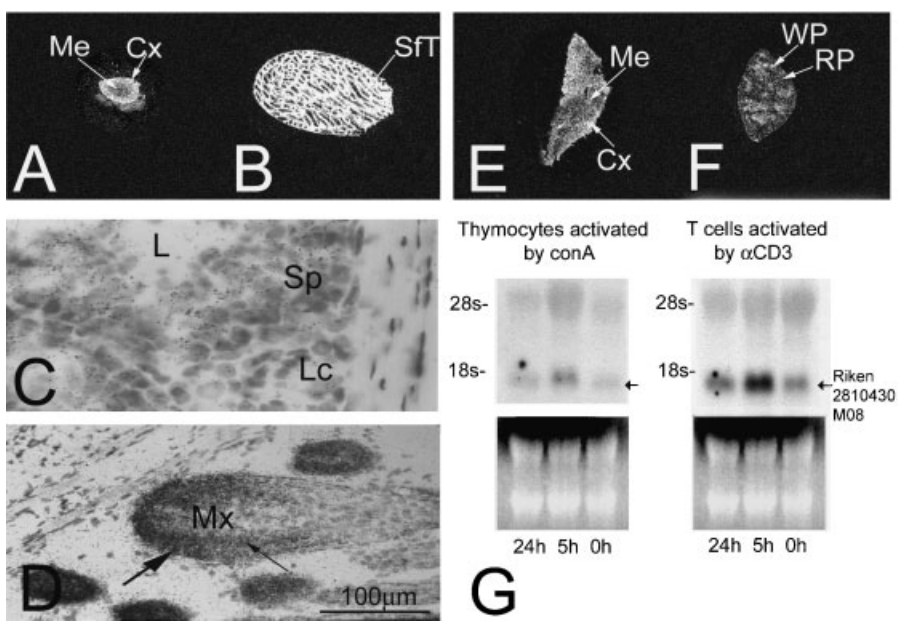

Fig. 3. Riken 2810430M08 expression in adult tissues. **A–F**: ISH of selected adult tissues for Riken 2810430M08 expression. A: Adrenal gland, Cx, cortex; Me, medulla. **B**, **C**: Testis, L, lumen; LC, Leydig cells; SfT, seminiferous tubules; Sp, spermatocytes. **D**: Skin, Mx, hair follicle matrix. The large and thin arrows indicate intensely labeled external and internal root sheaths, respectively. **E**: Thymus, Cx, cortex; Me, medulla. F: Spleen, WP, white pulp; RP, red pulp. **G**: Northern blot analysis of Riken 2810430M08 expression in thymocytes and T cells. Thymocytes were activated by Con A (1.5 μg/ml) and spleen T cells were activated by soluble anti-CD3 (0.1 μg/ml). The duration of activation is indicated. Arrows below the 18S position indicate the Riken 2810430M08 mRNA. Bands of 28S and 18S ribosomal RNA are presented to show RNA loading.

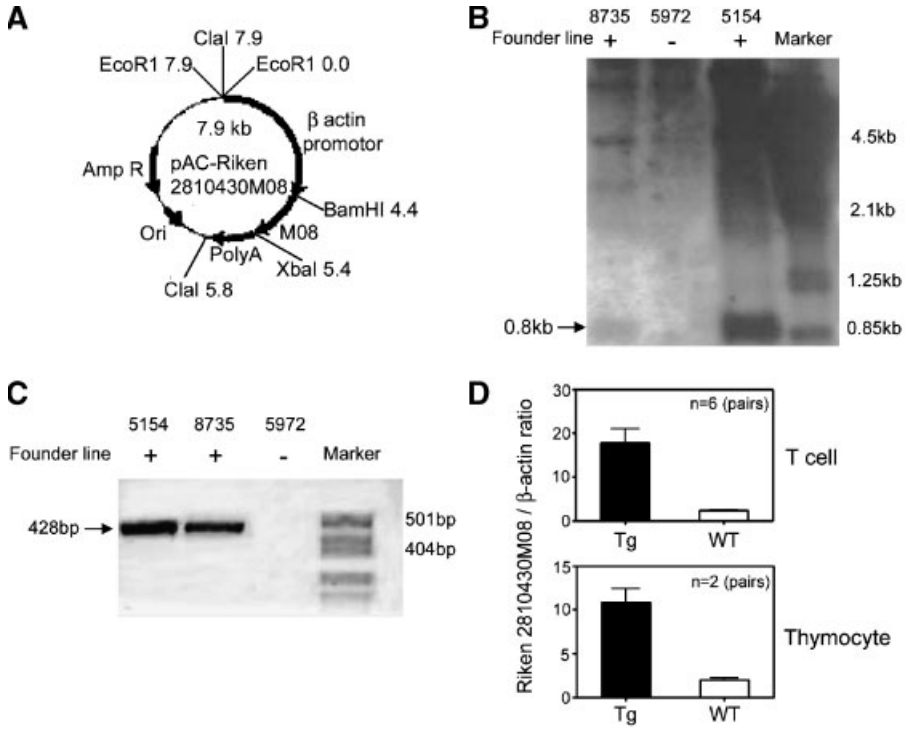

Fig. 4. Generation and characterization of Riken 2810430M08 Tg mice. **A**: pAC-Riken 2810430M08 construct for Tg mice generation. The 5.8-kb ClaI/ClaI fragment was used for microinjection. **B**: Genotyping of Riken 2810430M08 founder tail DNA by Southern blotting. The 0.8-kb bands specific to the Riken 2810430M08 transgene are indicated by an arrow. **C**: Genotyping of Riken 2810430M08 founder tail DNA by PCR. The 428-bp bands specific to the Riken 2810430M08 transgene are indicated by an arrow. **D**: Real-time RT-PCR of Riken 2810430M08 mRNA from spleen T cells and thymocytes. Mean ± SD of ratios of Riken 2810430M08 versus β-actin signals of Tg and WT mice are shown.

real-time RT-PCR in line 5154 Tg mice (Fig. 4D); similar data were obtained from line 8735 (data not presented). 2810430M08 mRNA expression in thymocytes was also increased according to real-time PCR (Fig. 4D).

Lines 5154 and 8735 were expanded for detailed study. These mice were fertile and manifested no gross anomalies upon visual inspection. Both lines had a similar phenotype in vitro and in vivo. Therefore, in most of the cases, unless specified otherwise, representative data for line 5154 are reported.

2810430M08 Tg Mice Present Normal Thymus and Spleen Cell Subpopulations

The thymus and spleen size and cellularity in adult 2810430M08 Tg mice were similar to those in WT mice (Fig. 5A). Flow cytometry analysis demonstrated normal percentage of $CD4^+CD8^+$ double-positive, $CD4^+$ single-positive, and $CD8^+$ single-positive subpopulations in the adult Tg thymus (Fig. 5B). T- versus B-cell and CD4- versus CD8-cell ratios in the spleen of adult Tg mice were comparable to those in WT controls (Fig. 5B). We wondered whether overexpression of 2810430M08 might affect thymocyte development in the embryonic stage, which was high in 2810430M08 expression according to our ISH study (Fig. 1). The fast-proliferating DN thymocytes were further divided into DN1 ($CD44^+CD25^-Lin^-$), DN2 ($CD44^+CD25^+Lin^-$), DN3 ($CD44^-CD25^+Lin^-$), and DN4 ($CD44^-CD25^-Lin^-$) subpopulations by flow cytometry, and these cells from E19 Tg and WT thymuses were compared; however, no discernable difference was observed (Fig. 5C).

In Vitro Tg T-Cell Function

Compared to WT T cells, expression of the T-cell activation markers CD25 and CD69 was normal in Tg T cells stimulated by anti-CD3, anti-CD3 plus anti-CD28, or PMA plus ionomycin (Fig. 6A).

We next examined cytokine production and Tg T cells proliferation. IL-2, IL-4, and IFN-γ secretion after anti-CD3 or anti-CD3 plus anti-CD28 stimulation in adult Tg T cells was

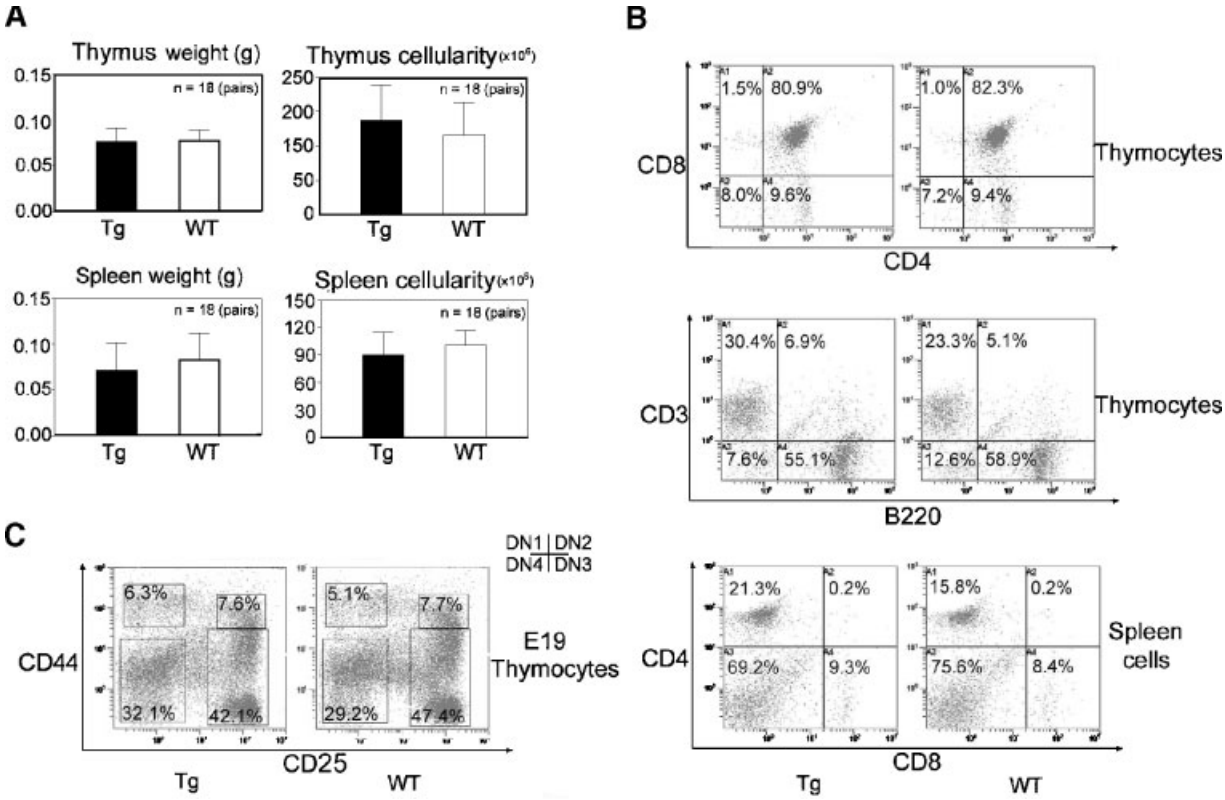

Fig. 5. Subpopulations of lymphocytes in Riken 2810430M08 Tg lymphoid organs. **A**: Weight and cellularity of the thymus and spleen. Eighteen pairs of Tg mice and their WT littermates were compared for their thymus and spleen weight and cellularity. Mean ± SD are shown. **B**: Cell subpopulations in the spleen. T-cell ($CD3^+$) and B-cell ($B220^+$) populations and CD4 and CD8 T-cell populations in the Tg and WT thymus and spleen were analyzed by two-color flow cytometry. The percentages are indicated in the histograms. The experiments were repeated more than three times, and representative data are shown. **C**: Double negative subpopulations in E19 thymi. Thymocytes from E19 fetuses were isolated and stained with Lin, CD25, and CD44 and analyzed by three-color flow cytometry for DN1, DN2, DN3, and DN4 subpopulations, the percentages of which were indicated in the histograms. Representative data from three pairs of Tg and WT thymi are shown.

comparable to that in adult WT T cells (Fig. 6B). Adult Tg T-cell proliferation stimulated by anti-CD3, anti-CD3 plus anti-CD28, or alloantigen was similar to that of WT T cells (Fig. 6C). In a few experiments and at a few time points, there was a moderate increase of Tg T-cell proliferation; however, we repeated the experiments for more than 10 times and this was not a consistent finding. To assess the role of this gene in proliferation of fetal cells, we isolated E19 thymocytes and E17 total embryonic cells and assayed their spontaneous proliferation. No significant difference was observed between Tg and WT cells (Fig. 6D). Adult Tg thymocytes had no apparent difference from WT thymocytes in terms of spontaneous or solid phase anti-CD3-stimulated proliferation and apoptosis (data not shown).

Chemotaxis of adult g LN cells towards SDF-1α showed no abnormality compared to WT cells, according to in vitro Transwell assays (Fig. 6E).

In Vivo Tg T-Cell Function

T-cell function in vivo was evaluated according to DTH, which is a T-cell-dependent reaction. In the response measured 1 week after FITC-skin priming, Tg and WT mice exhibited similar percentage of ear thickness increment (Fig. 7A).

Ig production, with the exception of the IgM isotype, is a T-cell dependent process. Different Ig isotypes, such as IgA, IgG1, IgG2a, IgG2b, IgG3, and IgE, in Tg and WT sera showed no statistically significant differences (Fig. 7B,C).

DISCUSSION

The human and mouse genome projects have provided us with overwhelming information,

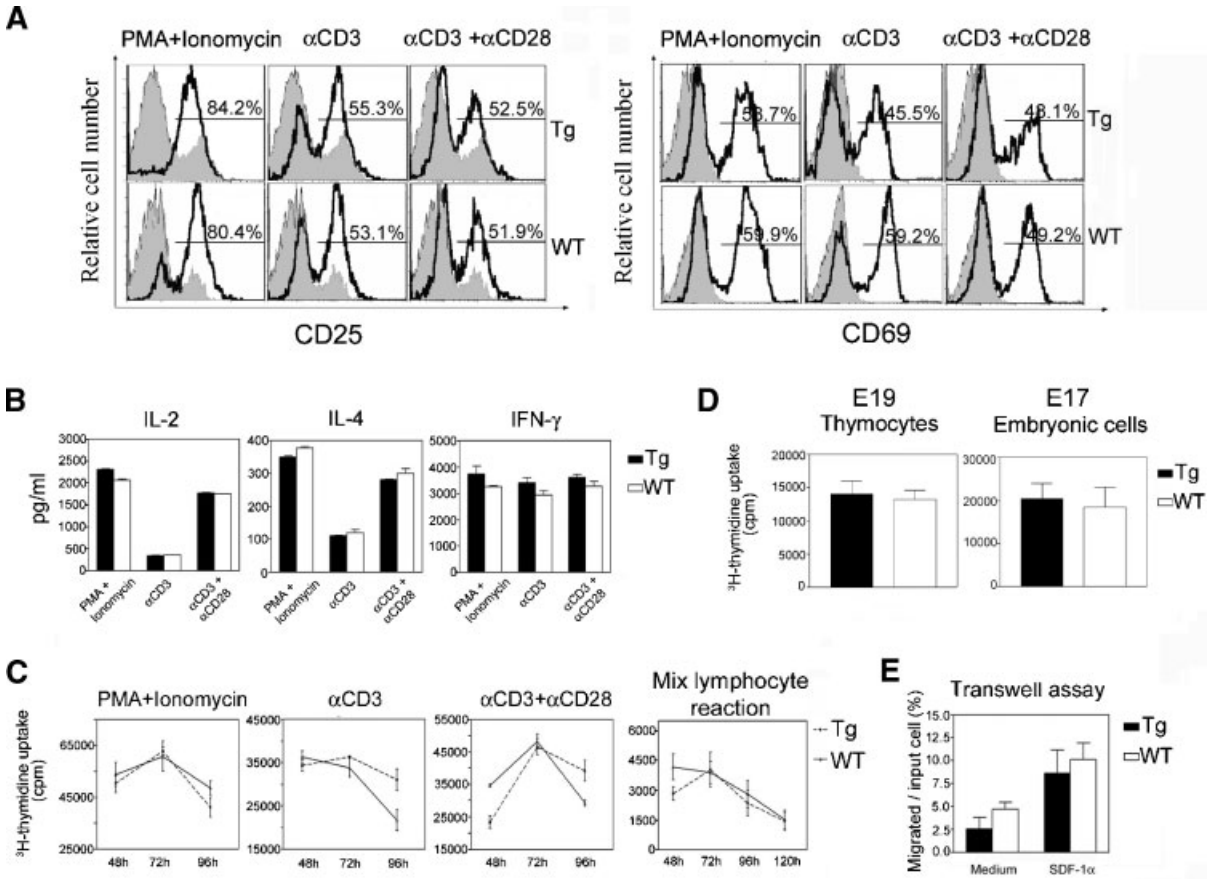

Fig. 6. In vitro assays of Tg T-cell functions. **A**: C69 and CD25 expression on activated T cells. Tg and WT T cells were stimulated overnight by solid phase anti-CD3 (4 μg/ml) or anti-CD3 plus anti-CD28 (0.57 and 2.86 μg/ml (concentrations used during coating), respectively). CD69 and CD25 expression on Thy-1.2-gated T cells was measured by two-color flow cytometry. Shadowed areas represent cells cultured in medium. **B**, **C**: Lymphokine production and proliferation of T cells. Tg and WT spleen T cells were stimulated by soluble PMA (10 nM) plus ionomycin (0.1 μg/ml), solid phase anti-CD3 (4 μg/ml), or solid phase anti-CD3 (0.57 μg/ml) plus anti-CD28 (2.86 μg/ml), as indicated. In mixed lymphocyte culture, total spleen cells from Tg or WT mice were stimulated by mitomycin C-treated allogeneic BALB/c spleen cells. Supernatants were harvested on the days indicated and assayed for lymphokines by ELISA (Fig. 5B). ^{3}H-thymidine uptake of the remaining cells was measured in triplicate (Fig. 5C). Mean ± SD of cpm are shown. **D**: Proliferation of fetal thymocytes and total fetal cells. E19 fetal thymocytes (left **panel**) and E17 total fetal cells (right **panel**) were isolated and cultured at 0.4×10^{5}/200 μl/well for 20 h. ^{3}H-thymidine uptake during this period was measured. Data were derived from three pairs of Tg and WT fetuses. **E**: Migration of lymph node (LN) cells towards SDF-1α. Mean ± SD of percentage of LN cell migration towards SDF-1α in the lower chamber of the Transwell are registered. Samples were in duplicate. The experiments were repeated more than three times, and representative data are shown.

among which is a large group of genes with no known function, and not containing discernable homology to the functional domains of other genes. We thus face a daunting task to elucidate the biological roles of these genes. In the present study, we took two approaches to this end for Riken 2810430M08, which was selected due to its upregulation during T-cell activation. First, ISH was employed to map its expression during ontogeny and in adulthood. Subsequently, Tg mice with actin promoter-driven universal 2810430M08 expression were generated to explore the function of this gene, with emphasis on the immune system.

According to our in situ study, 2810430M08 presented a pattern of temporal expression, peaking in the mid-gestation (e9–e14) stage when it was transcribed at high levels in most tissues. Its expression declined in most tissues afterwards, suggesting that this gene might have important roles in fetal development during the mid- but not the late-gestation stage, whereas its expression during the early stage of development remains to be determined.

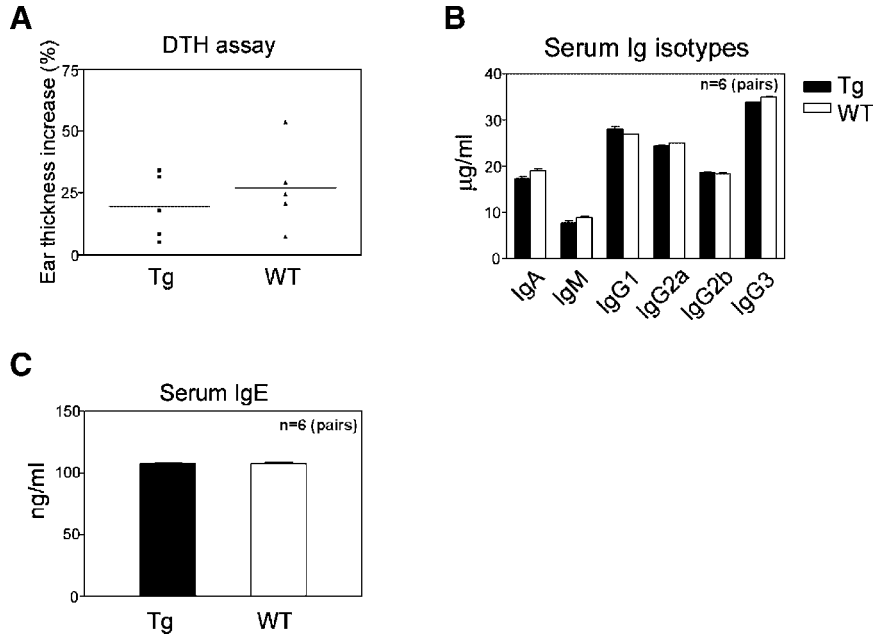

Fig. 7. In vivo Tg lymphocyte functions. **A**: DTH assay. Five pairs of Tg mice and their WT littermates were compared for ear thickness increase after FITC challenge. Horizontal bars represent the mean percentage increase calculated as follows. % increase = (Mean ear thickness 24 h after ear painting with FITC−mean ear thickness before ear painting)/mean ear thickness before ear painting. **B**, **C**: Mouse serum immunoglobulin levels. Mean ± SD of concentrations of serum IgA, IgM, IgG1, IgG2a, IgG2b, IgG3 (B), and IgE (C) in Tg and WT mice (n = 6 pairs) are shown. Samples were assayed in duplicate.

In the late-gestation stage and during adulthood, 2810430M08 was expressed in some tissues and cells with a robust proliferation program, such as thymocytes, activated T cells, root sheaths of hair follicles, and Sp, suggesting that this gene might have proliferation-related functions. On the other hand, 2810430M08 was also expressed in certain areas of the central and peripheral nervous system in adults, such as pyramidal neurons layer of CA1 in the hippocampus, granule neuron of DG, amygdales and mammillary bodies, and gray matter of the spinal cord, none of which contains vigorously proliferating cells. Thus, this gene might also have important neuronal functions not related to proliferation.

In adulthood, relatively high-level transcription of 2810430M08 occurred in the adrenal cortex, pointing to its possible involvement in cortical steroid synthesis.

Postnatally, 2810430M08 was expressed at relatively high levels in the thymus, and to a lesser extent, in the spleen. Its expression was induced 5 h after TCR stimulation in T cells. All these results suggest a role for this gene in T-cell immune responses. However, when the gene was overexpressed in Tg mice, according to all the tests we performed in vitro and in vivo, the T cells seemed to show no anomaly in terms of activation, lymphokine secretion, proliferation, migration, and in vivo DTH. As this gene is expressed in the fetus, we assessed the proliferation of fetal thymocytes and total fetal cells, but no apparent difference was observed between Tg and WT cells. Also, subpopulation percentages in the fast-proliferating fetal thymus DN cells were similar in Tg and WT fetuses.

There could be several explanations for such observations. Most likely, endogenous 2810430 M08 expression was more than sufficient for T-cell functions; therefore, the increased expression in Tg T cells minimally further influenced the function of this gene. It is also possible that the approximate threefold rise in 2810430M08 expression in Tg T cells was not sufficient to disturb T-cell biology. Last, we cannot rule out that there are undiscovered abnormal functions in immune and other systems of Tg mice.

ACKNOWLEDGMENTS

The authors thank Mr. Ovid Da Silva for his editorial assistance, Dr. Martin Marcinkiewicz

for ISH analysis, and the Core Facility of the New Emerging Team of Transplantation for DNA microarray analysis. This work was supported by grants from Canadian Institutes of Health Research (CIHR, MOP57697 and MOP69089), the Kidney Foundation of Canada, the Heart and Stroke Foundation of Quebec, the Juvenile Diabetes Research Foundation, USA (1-2005-197), and the J.-Louis Levesque Foundation to J.W. Group grants from the CIHR for New Emerging Teams in Transplantation and from Fonds de la recherche en santé du Québec (FRSQ) for Transfusional and Hemovigilance Medical Research are also acknowledged. J.W. is a National Scholar of the FRSQ. The work was also supported by a CIHR grant (MOP79565) to H.L.

REFERENCES

Luo HY, Yu G, Tremblay J, Wu JP. 2004. EphB6-null mutation results in compromised T cell function. J Clin Invest 114:1762–1773.

Marcinkiewicz M. 2002. BetaAPP and furin mRNA concentrates in immature senile plaques in the brain of Alzheimer patients. J Neuropathol Exp Neurol 61:815–829.

Shi GX, Wu YL, Zhang J, Wu JP. 2003. Death decoy receptor TR6/DcR3 inhibits T cell chemotaxis in vitro and in vivo. J Immunol 171:3407–3414.

Terra R, Louis I, Le Blanc R, Ouellet S, Zuniga-Pflucker JC, Perreault C. 2005. T-cell generation by lymph node resident progenitor cells. Blood 106(1):193–200.